見頻度が高いことがわかった[1]．重松らは43万人中8人（1/5.3万人）[2]，坂本らは約42,500人中5人（1/8,500人）[3]に発見されたと報告している．厚生労働省研究班のパイロットスタディによるとプロピオン酸血症は約5万人に1人で，タンデムマス法の対象疾患では最も頻度が高い．本症では大部分が乳児期早期に嘔吐などの急性症状で発症し，予後不良の疾患と考えられているが，外国と異なり日本人の患者では，無症状のいわゆる軽症型プロピオン酸血症が多いことも分かってきた．

プロピオン酸血症の欠損酵素は，プロピオニルCoAカルボキシラーゼ（PCC）であるが，この酵素はα，βの2つのサブユニットからなるヘテロ二量体であり，それぞれのサブユニットは*PCCA*，*PCCB*遺伝子にコードされている[4]．日本人の軽症型プロピオン酸血症では*PCCB*遺伝子のY435C変異の頻度が高く，そのアリル頻度からホモ接合体頻度は約1/30,000と計算されている[1]．また，その他の稀な変異がPCCB遺伝子のみならずPCCA遺伝子にも知られている[5]．

重症型プロピオン酸血症は，乳児期早期から高アンモニア血症，代謝性アシドーシスなどを呈し，治療用特殊ミルクを併用した食事療法と，L-カルニチン，メトロニダゾールなどで治療される[6]．軽症型症例でも同様の治療をしている報告がある[7]．しかし，軽症型プロピオン酸血症に治療が必要かどうかについてはまだ不明である．そこで今回我々は，新生児MSで発見されたプロピオン酸血症患者のC3やMC，3HPAなど代謝産物の変化を追跡し，治療やフォローアップなどの必要性について検討した．

【方　法】

2004年から2009年までの期間中に島根大学で行ったタンデムマスによる新生児MSで，C3又はC3/C2の上昇がみられ，尿中有機酸分析でMCや3HPAの上昇，または遺伝子検査で確定診断されたプロピオン酸血症の6症例を検討した（表1）．尿中有機酸分析はGC/MSを用いて既報の方法に準じて行い[8]，また臨床経過と異常代謝産物の推移を観察した．

【結　果】

今回検討したプロピオン酸血症6例（男：女＝3：3）の最終追跡年齢は1ヶ月～4歳1ヶ月であっ

表1．プロピオン酸血症の新生児期の所見とその他の情報

症例	軽症				重症		基準値
	1	2	3	4	5	6	
性別	男	男	女	女	男	女	
最終調査時年齢	4y1m	1y4m	8m	1y0m	1m	1m	
尿中有機酸（%;内部標準とのピーク面積比）							
MC	1.88	2.98	1.69	4.07	142.4	48.5	(<1.1)
3HPA	1.38	nd	5.12	6.44	384.4	967.7	(<1.1)
ろ紙血アシルカルニチン（μM）							
C3	4.6	4.25	9.43	6.98	12.9	15.2	(<5.25)
C3/C2	0.24	0.23	0.18	0.29	1.53	2.59	(<0.2)
C0	46.1	20.7	62.7	15.9	8.08	4.43	(10～60)
	R77W/unknown (PCCA)	Y435C/Y435C (PCCB)	NA	Y435C/unknwon (PCCB)	NA	NA	

略語：MC＝メチルクエン酸；3HPA＝3ヒドロキシプロピオン酸；nd＝not determined；NA＝not analysed；nd=not detected(<0.1)
基準値は新生児期のもの
アンダーラインは異常値を示す

た．新生児重症型（古典型）の症例5，6は1ヶ月間のみ追跡した．初回の検査結果は表1に示すように，軽症型の症例1～4ではMC，3HPAの上昇は軽度で，臨床症状を認めなかった．症例5，6はMC，3HPAが非常に高く，出生直後には既に嘔吐や哺乳不良等の症状が出現していた．遺伝子解析を行った軽症型3例の結果は，症例1では*PCCA*遺伝子のR77W/unknown，症例2ではPCCB遺伝子のY435Cのホモ接合体，症例4ではY435C/unknownであった．

軽症型プロピオン酸血症4例の血中アシルカルニチン所見は，C3上昇のみが1例，C3/C2上昇のみが2例，C3，C3/C2の両方が上昇した例は1例であった．C0は新生児ろ紙血の正常範囲内にあった．また尿中有機酸分析では，症例2でMCの上昇のみが認められ，他の3症例ではMCのみならず3HPAの排泄増加もみられた．

一方，新生児発症の重症型（症例5，6）の2例では，軽症型に比べ，C3が高く，遊離カルニチンの低下が他の4症例に比べて顕著であった．さらにC3/C2は軽症型症例の5倍以上であった．尿中有機酸分析所見ではMCも3HPも他の4例に比べ数十倍の増加が見られた

軽症型プロピオン酸血症4例のMC，3HPA，C3，C3/C2の推移をそれぞれ図1～4に示した．

1）MC：症例1と3では漸減し正常範囲またはボーダーラインに低下した．症例2と4では，少なくとも1年以上，MCの高値が持続した．

2）3HPA：症例1は2歳時に一過性の上昇を認めたが，特に症状なく経過した．症例2，3，4はカットオフを超える値が持続し，特に症例2，4は最終追跡時点（1年以上）でも高値を示した．

3）C3：症例1と3は，最初の再検査の時から正常値を示していた．症例2は，初回は正常値であったが次第に上昇し，高値が継続した．症例3は，初回は異常値であったが5ヶ月に検査した後は正常範囲にあった．症例4では高値を示した．これまでのところ軽症型症例は全例（症例1～4）無治療で，明らかな代謝異常を思わせるような症状はみられず，正常に発達している．

4）C3/C2：症例1は最初の検査では異常値であったが，2回目以降は正常だった．症例3，4は初回から正常値を維持していた．症例2は異常値と正常値を交互に示している．

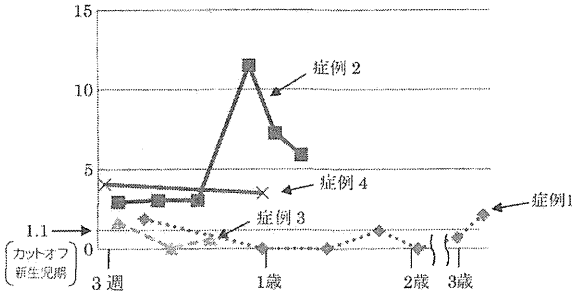

図1．メチルクエン酸（MC）の推移

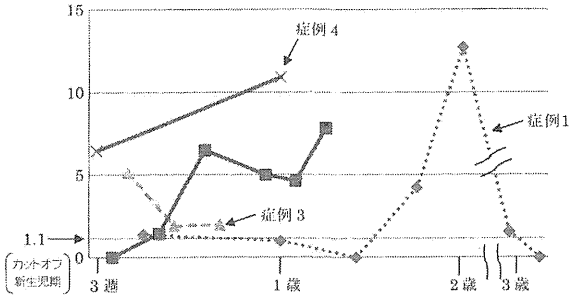

図2．3ヒドロキシプロピオン酸（3HPA）の推移

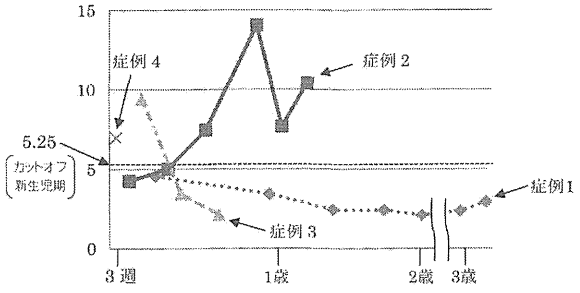

図3．プロピオニルカルニチン（C3）の推移

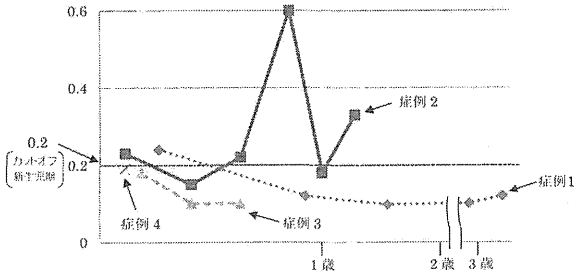

図4．C3/C2の推移

またC0については，初回のMS/MSにおいて全症例で正常値であり，2回目以降についても新生児期以降の正常値である20μM以上を示していた．

【考　察】

今回検討した軽症型プロピオン酸血症4例では，全例で尿中MCの上昇により本症と化学診断され，1例はY435C変異がホモでみられた．一方，新生児発症の重症型2例では，尿中有機酸異常所見が他の軽症型4症例に比べて著しい異常を示したことから，生化学的に重症型の区別は容易であると思われる．

アシルカルニチン所見では，初回分析でC3，C3/C2のいずれも上昇していたのは症例4のみで，他の3例はC3，C3/C2のいずれかの異常を示しただけであった．C3，C3/C2どちらかの異常があればプロピオン酸血症の可能性が高く，尿中有機酸分析などの精査を進める必要性があることを示唆する．

異常代謝産物の量の推移をみると，症例1，3では有機酸分析でMC，3HPA，C3の量は新生児期のカットオフ値以下に低下したが，症例2，4では少なくとも1年以上は異常値が持続した．後者の2例ではいずれもY435C遺伝子変異をもつタイプであった．

症例1では2歳時に3HPAの一過性の再上昇が認められたが，MCの上昇は軽度であった．この採尿時に患児が便秘症を呈していたことがわかっており，腸内細菌が3HPAの再上昇に影響を与えた可能性や，タンパク摂取量によっても影響されると考えられる．

今回検討した軽症型プロピオン酸血症は4例全例が無治療でこれまでのところ明らかな症状は認められていない．軽症型プロピオン酸血症であれば，特別な治療は必要ないと考えられるが，軽症プロピオン酸の患児から検出され続ける限りは，半年～1年に1回のフォローが必要であろう．現時点では，新生児MSで軽症型プロピオン酸血症と診断され，その後に重症化した症例の報告はないが，長期予後に関してはまだ不明な点が多いからである．

一方，新生児期には無症状で乳児期に嘔吐や哺乳不良などの症状で発症した重症型プロピオン酸血症の症例は数多く報告されている[9),10),11)]．今回の症例2，4のような異常代謝産物の値に改善がみられない例では，将来急性増悪する危険性は否定できない．特にY435Cに遺伝子変異をもつ症例については日本人患者で頻度の高い変異だけに，定期的なタンデムマス分析や尿中有機酸分析，また適宜，心電図検査や脳MRI検査を行う必要がある[5)]．症例2と4のような症例では日常生活において，シック・デーには状態を注意深く観察し，嘔吐や哺乳不良，傾眠傾向などの症状を伴う際にはすみやかにアシドーシスやアンモニアなどのチェックをする必要がある．これらの生活上の注意点を，両親に十分に説明しておくことを念頭に置いておくべきである．

今後，タンデムマスによる新生児MSの普及とともに，今回のような軽症型の代謝異常症や，メチルクロトニルグリシン尿症のように大部分が無症状と考えられているような症例の発見頻度は増加すると予想される．無症状の疾患の長期予後については，軽症型イソ吉草酸尿症の治療指針があるのみで[12),13)]その他の軽症型疾患について明確な治療指針はない．今後，マス・スクリーニングの普及と同時に長期追跡を通して，エビデンスに基づいた軽症型に対する指針を作成する必要がある．

文　献

1) Yorifuji T et al. Unexpectedly high prevalence of the mild form of propionic acidemia in Japan: presence of a common mutation and possible clinical implications. Hum Genet. 111: 161-165, 2002
2) 重松陽介：広がり始めたタンデムマス・スクリーニングの現況　日本マススクリーニング学会誌　17: 19-24, 2007
3) 坂本　修ら：新生児タンデムマススクリーニングで発見されるC3，C3/C2高値例の検討　日本マス・スクリーニング学会誌　19: 63-68, 2009

4) Yang X et al. Mutation spectrum of the PCCA and PCCB genes in Japanese patients with propionic acidemia. Mol Genet Metab. 81: 335-342, 2004
5) 重松陽介：タンデムマス・スクリーニングにおける直接精密検査と診断確定の重要性　特殊ミルク情報　44: 57-59, 2008
6) 特殊ミルク共同安全開発委員会　タンデムマス導入にともなう新しいスクリーニング対象疾患の治療指針　特殊ミルク情報　42: 10, 2006
7) 長尾雅悦：タンデムマススクリーニングによって発見された軽症型プロピオン酸血症の診断と治療　小児科　50: 651-655, 2009
8) Kimura M et al. A personal computer-based system for interpretation of gas chromatography mass spectrometry data in the diagnosis of organic acidaemias. Ann Clin Biochem. 36: 671-672, 1999
9) Johnson JA et al. Propionic acidemia: case report and review of neurologic sequelae. Pediatr Neurology. 40: 317-320, 2009
10) Lücke T et al. Propionic acidemia: unusual course with late onset and fatal outcome. Metabolism. 53: 809-810, 2004
11) 鎌田彩子ら：プロピオン酸血症の1例－診断後16年間にわたる治療経過について－　小児科臨床　57: 959-962, 2004
12) Ensenauer R et al. A common mutation is associated with a mild, potentially asymptomatic phenotype in patients with isovaleric acidemia diagnosed by newborn screening. Am J Hum Genet. 75: 1136-42. 2004
13) Vockley J, et al. Isovaleric acidemia: new aspects of genetic and phenotypic heterogeneity. Am J Med Genet C Semin Med Genet. 142: 95-103. 2006

受付日：平成24年10月31日
受理日：平成24年12月19日

▷第59回学術集会　シンポジウム7：臨床検査への質量分析の応用(4)◁

小児科領域におけるタンデムマスとGC/MSの臨床応用：最近の進歩

山　口　清　次*

Clinical Application of Mass Spectrometry in the Pediatric Field: Current Topics

Seiji YAMAGUCHI, MD*

Mass spectrometry, including tandem mass spectrometry (MS/MS) and gas chromatography-mass spectrometry (GC/MS), is becoming prominent in the diagnosis of metabolic disorders in the pediatric field. It enables biochemical diagnosis of metabolic disorders from the metabolic profiles obtained by MS/MS and/or GC/MS. In neonatal mass screening for inherited metabolic disease (IMD) using MS/MS, amino acids and acylcarnitines on dried blood spots are analyzed. The target diseases include amino acidemia, urea cycle disorder, organic acidemia, and fatty acid oxidation disorder. In the MS/MS screening, organic acid analysis using GC/MS is required for differential and/or definite diagnosis of the IMDs. GC/MS data processing, however, is difficult, and metabolic diagnosis often requires the necessary skills and expertize. We developed an automated system of GC/MS data processing and autodiagnosis, and the biochemical diagnosis using GC/MS became markedly easier and user-friendly. Mass spectrometric techniques will expand from research laboratories to clinical laboratories in the near future. 【Review】

[Rinsho Byori **61**：817～824, 2013]

Corresponding author: *Seiji YAMAGUCHI*, MD, Department of Pediatrics, Shimane University School of Medicine, Izumo 693-8501, Japan. E-mail: seijiyam@shimane-med.ac.jp

【Key Words】 tandem mass spectrometry（タンデムマス），gas chromatography-mass spectrometry: GC/MS（ガスクロマトグラフ質量分析計），organic acidemia（有機酸代謝異常症），fatty acid oxidation disorder（脂肪酸代謝異常症），neonatal mass screening（新生児マススクリーニング）

質量分析は，生体試料中の微量物質を高感度・高精度に網羅的分析が可能な機器である。微量の検体で同時に多くの情報が得られるため，メタボロミクス，プロテオミクス解析に応用されている。従来質量分析は，もっぱら研究室で使われていたが，最近臨床検査として使われるようになりつつある。

小児科領域では，代謝異常の診断に質量分析が普及しつつある。なかでも，「ガスクロマトグラフィー質量分析法(GC/MS)による先天代謝異常症の診断」と「タンデム型質量分析(タンデムマス)によるアシルカルニチン分析」は，条件付きではあるものの最近保険収載された。さらに最近ガスリー血液ろ

*島根医科大学小児科（〒693-8501 出雲市塩冶町89-1）

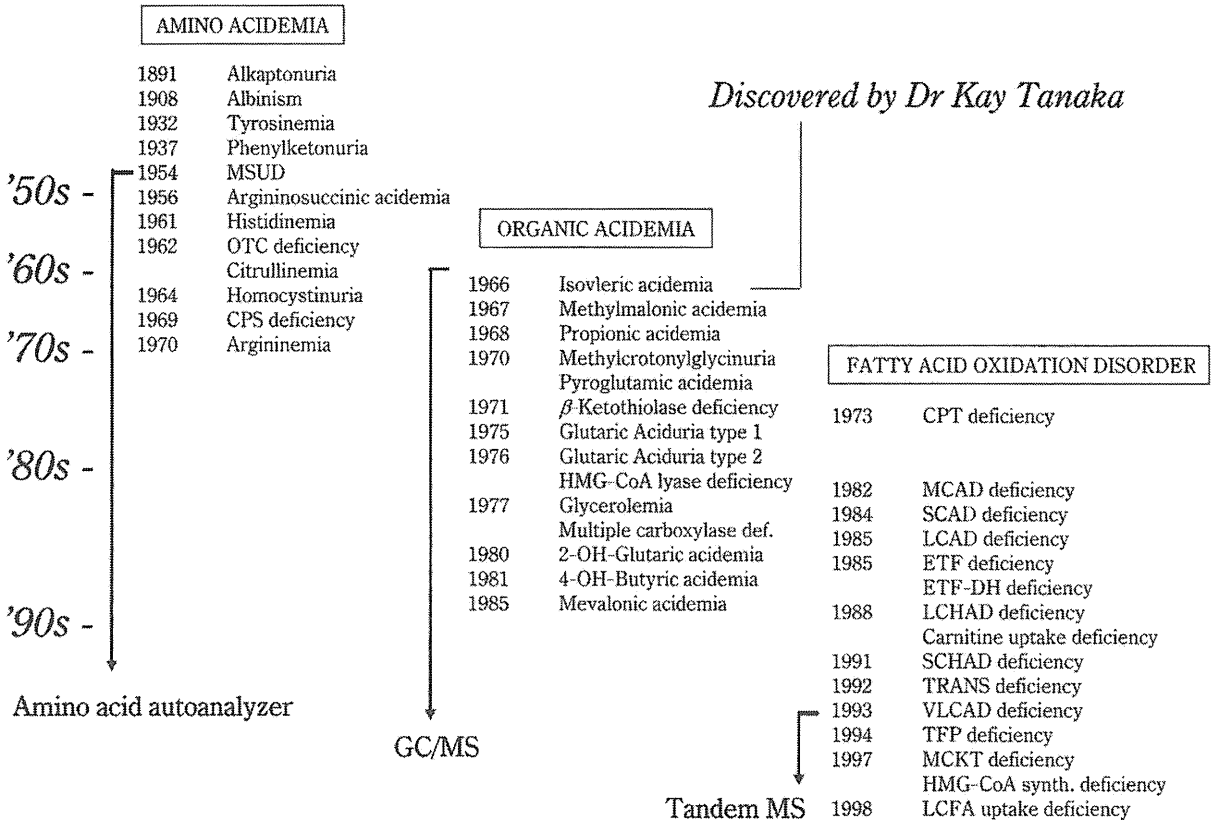

Figure 1 Discovery of amino, organic and fatty acid oxidation disorders.

紙を用いる新生児マススクリーニングにタンデムマス法が導入されるようになり，質量分析の臨床応用が広がりつつある[1)2)]。そこで小児科領域で普及しつつある質量分析による代謝異常の診断について述べたい。

I. 代謝異常診断における質量分析の臨床応用の歴史背景

アミノ酸・有機酸・脂肪酸代謝異常症の発見の歴史と分析機器の発達との関連性を **Fig. 1** に示している。

A. アミノ酸代謝異常症

食物や体蛋白異化に由来するアミノ酸の代謝障害のために，体液中にアミノ酸が増加する疾患である。1900 年頃にアルカプトン尿症，白子症などを例に挙げて「先天代謝異常症」の概念が提唱されて以来，1932 年にチロシン血症，1934 年にフェニルケトン尿症，1954 年にメープルシロップ尿症などのアミノ酸代謝異常症が発見された。1950 年代にアミノ酸自動分析計が開発され現在知られているほとんどのアミノ酸血症が同定された。そして 1960 年代に尿素回路異常症が同定された。

B. 有機酸代謝異常症

1966 年に K. Tanaka らが GC/MS によってイソ吉草酸血症を同定し報告したのが最初である。以後同様の手法で，1967 年メチルマロン酸血症，1968 年プロピオン酸血症が発見され，1970 年代を中心に主な有機酸代謝異常症が同定された。

C. 脂肪酸代謝異常症

1970 年代にカルニチンパルミトイルトランスフェラーゼ(CPT)欠損症が同定されていたが，あまり注目されていなかった。1982 年に突然死症例から中鎖アシル-CoA 脱水素酵素(MCAD)欠損症が同定されて以来，小児の突然死との関連に注目されるようになり研究が発展した。そして 1990 年台にタンデムマス法が開発され，生化学診断が著しく簡単になり，現在ではタンデムマス法を導入した新生児マススクリーニングが普及しつつある[3)]。

Table 1 Clinical features of amino acidemia, urea cycle disorder, organic acidemia, and fatty acid oxidation disorder, and biochemical diagnosis

Clinical features	Tools for biochemical diagnosis
Amino acidemia	
・Neurological impairment ・Convulsion, unconsciousness ・Liver dysfunction ・Renal stone	Amino acid analysis (Organic acid analysis)
Urea cycle disorder	
・Convulsion, unconsciousness ・Mental retardation ・Hyperammonemia	Amino acid analysis Blood ammonia Organic acid analysis
Organic acidemia	
・Acute onset with hypotonia, unconsciousness from early infancy ・Intermittent episodes of ketosis, hypoglycemia ・Neurological retardation ・Other (ex. intractable eczema)	Organic acid analysis Acylcarnitine analysis
Fatty acid oxidation disorder	
・Lethargy, hypotonia, myalgia ・Acute encephalopathy, sudden death ・Cardiomyopathy ・Non-ketotic hypoglycemia ・Liver dysfunction, CK elevation	Acylcarnitine analysis Organic acid analysis

II. アミノ酸・有機酸・脂肪酸代謝異常症の臨床的特徴

Table 1 に示すように，アミノ酸代謝異常症は血液(または尿)のアミノ酸分析，尿素回路異常症では血中アンモニア値とアミノ酸分析などによって診断される。有機酸代謝異常症と脂肪酸代謝異常症は，GC/MS による尿中有機酸分析，タンデムマスによる血中アシルカルニチン分析によって生化学診断される。両者ともカルボン酸の増加する点で類似しているが臨床的特徴に違いがみられる。前者は有機酸の臓器毒性の所見がみられることが多く，後者はエネルギー産生不全による症状が前面に出る。

タンデムマス法ではアミノ酸とアシルカルニチン分析が可能であり，これら上記4種類の疾患群のスクリーニングに用いられる。GC/MS による尿中有機酸分析では，有機酸代謝異常症の生化学診断に最も威力を発揮するが，一部のアミノ酸血症でも補助的診断に用いられる。例えば，有機酸分析によって，フェニルケトン尿症でフェニルピルビン酸やフェニル乳酸，メープルシロップ尿症で分枝鎖 α ケト酸の増加が観察される。尿素回路異常症では，一部の疾患でウラシル，オロット酸の増加がみられ診断に有用である。さらに脂肪酸代謝異常症の家長鎖脂肪酸代謝異常症では非ケトン性ジカルボン酸尿症がみられ，中鎖アシル-CoA 脱水素酵素欠損症ではヘキサノイルグリシンやスベリルグリシンのような診断的に有用な有機酸が検出される。

III. タンデムマスと GC/MS について

A. タンデムマス

MS が直列に並んだ構造(MS1 と MS2)構造を持ち，MS1 と MS2 で測定された粒子の質量数を比較して分子量が推定される。そしてそれぞれの分子のイオン強度によって定量される。非常に高感度な分析が可能であり[4]，新生児マススクリーニングでは，血液ろ紙の 3mm 大のディスクでよく，血清 10μL で分析可能である[5]。また分析試薬等がキット化され前処理も非常に簡単になっている。1検体の分析時間は2分程度であり，ランニングコストも安価なた

め，マススクリーニングに向いている。

タンデムマスでは，アミノ酸とアシルカルニチンが同時分析される。アミノ酸に関しては，アミノ酸分析計に比べると精度が低く限られたアミノ酸のみが測定可能である。このため代謝異常スクリーニングに用いられる。一方アシルカルニチン分析では，遊離カルニチン(C0)とアシルカルニチンが測定され，有機酸代謝異常症や，脂肪酸β酸化異常症(脂肪酸代謝異常症)の診断，スクリーニングに応用される。定性のための情報はイオンの質量数のみであるため，異性体の分離測定が困難である。しかしアシルカルニチンプロフィールが得られるため，後述のGC/MSに比べて，脂肪酸代謝異常症の診断には非常に有用である。

B. GC/MS

ガスクロマトグラフ(GC)と質量分析計(MS)が連結した構造を持つ機器である。GC分析するためには揮発性の物質に変える必要があるので，生体試料から抽出した物質を誘導体化してGC分析する[6]。GCから出てきた粒子は電子衝撃イオン化法で断片化されMSに導入される。マススペクトルは，分子構造の情報となる断片イオンが比較的多いため，異性体の同定も可能である。分析項目は尿中有機酸分析である。有機酸は弱酸であり体内に増加すると直ちに尿中に排出されるため尿の分析が用いられる。MSで一斉分析し，有機酸全体のプロフィールから代謝障害部位が特定される。

タンデムマスに比べGC/MSでは，機器のメンテナンスには比較的熟練を要し，また前処理も手間がかかり，分析時間も30～60分程度かかることが多い。しかし，詳細な代謝プロフィールが得られ，代謝異常の同定のみならず，乳酸ピルビン酸の増加，ケトーシス，ジカルボン酸尿症など患者の一過性の状態を把握することができ，病態評価，治療評価などに向いている。

IV. 質量分析による代謝異常症の生化学診断

体内に代謝障害があると，障害部位の上流物質とそれに由来する異常代謝産物がMSによる一斉分析で検出される。タンデムマスとGC/MSの分析プロフィールから，代謝障害部位が推定される。主な疾患とタンデムマスとGC/MS分析における診断マーカーを**Table 2**にあげた。

A. GC/MSによる尿中有機酸分析による生化学診断

ロイシンの代謝過程と有機酸代謝異常症を**Fig. 2**に例示している。最下段のメチルマロン酸血症では，メチルマロニル-CoAムターゼ欠損によって，methylmalonateとともにその上流のプロピオニル-CoAの代謝産物(methylcitrate，3-OH-propionate，propionylglycine等)が増加する。このプロフィールから生化学診断する。

その上流のプロピオン酸血症では，propionyl-CoA由来の状代謝産物との上流の2-methyl-3-OH-butyrate，tiglylglycine等が増加し，この特徴的なプロフィールから生化学診断される。

さらに，プロピオン酸血症の上流のβケトチオラーゼ欠損症では，上流の2-methyl-3-OH-butyrateやtiglylglycineが増加し，一方下流のpropionyl-CoA由来の代謝産物の増加はみられない。

B. タンデムマスによるアシルカルニチン分析

Fig. 2に示す3疾患のアシルカルニチン分析所見は，メチルマロン酸血症とプロピオン酸血症ではC3(propionylcarnitine)の増加がみられる。βケトチオラーゼ欠損症ではC5:1(tiglylcarnitine)とC5-OH(2-methyl-3-OH-butyrylcarnitine)の増加がみられる。メチルマロン酸血症とプロピオン酸血症は両疾患ともにC3の上昇しか見られないため，GC/MSによる尿中有機酸分析によって鑑別しなければならない。

V. GC/MSデータ自動解析・自動診断プログラム

GC/MS分析では，ガスクロマトグラムに相当するTIC(total ion current)が得られるが，この段階では，ピークの情報はピーク保持時間のみである。そのあと質量分析されると，各ピークのマススペクトルが得られる。**Fig. 3**にプロピオン酸血症の尿中有機酸分析所見とマススペクトルを例示している。しかし尿中に含まれる有機酸は数百以上あるので，すべてのピークをマススペクトルで同定してピーク強度などで定量することは，時間がかかるうえに，極めて困難な作業である。さらに代謝産物とその量がわかっても，代謝異常症に関する知識を必要とし，GC/MSデータをマニュアルで解析して生化学診断をすることは，専門知識のみならず，時間と労力を要する。

そこで我々は，独自に「GC/MSデータ自動解析・自動診断プログラム」を開発した[7]。これを使えば，GC/MS分析後に数分以内に，異常代謝産物を検出

Table 2 Main target diseases detectable by MS/MS and diagnostic markers

Disease	Diagnostic marker	
	MS/MS*	GC/MS**
Amino acidemia		
Phenylketonuria	Phe	PPA, PLA
Maple syrup urine disease	Ileu, Leu, Val	2KIV, 2M3VA, 2KIC
Homocystinuria	Met	—
Urea cycle disorder		
Citrullinemia (type I)	Cit	Orot, Uracil
Argininosuccinic aciduria	Cit (ASA)	Orot, Uracil
Organic acidemia		
Methylmalonic acidemia	C3, C3/C2	MMA, MC, 3HPA, PG
Propionic acidemia	C3, C3/C2	MC, 3HPA, PG
Isovaleric acidemia	C5	IVG
Methylcrotonylglycinuria	C5-OH	MCG, 3HiVA
HMG-CoA lyase deficiency	C5-OH	HMGA, MGA, MGCA
Multiple carboxylase deficiency	C5-OH	MC, MCG, 3HPA
Glutaric acidemia type I	C5-DC	GA, 3HGA
β-ketothiolase deficiency	C5-OH, C5:1	2M3HBA, TG
Fatty acid oxidation disorder		
MCAD deficiency	C8	HG, SG
VLCAD deficiency	C14:1	DIC
TFP deficiency	C16-OH, C18-OH	DIC, 3HDIC
CPT-1 deficiency	C0/[16+C18]	DIC
CPT-2 deficiency	(C16+C18:1)/C2, C16	DIC
Primary carnitine deficiency	C0 (reduced)	DIC
Glutaric acidemia type II	C8, C10, C12, etc	DIC, EMA, IVG, GA, etc

*MS/MS, amino acid and acylcarnitine in blood; GC/MS, urinary organic acid.
Abbreviations: MCAD and VLCAD, medium-chain- and very-long-chain-acyl-CoA dehydrogenases, respectively; TFP, mitochondrial trifunctional protein; CPT-1 and CPT-2, carnitine palmitoyltransferase-I and -II, respectively; PPA, phenylpyruvate; PLA, phenyllactate; 2KIV, α-ketoisovalerate; 2M3VA, α-keto-3-methylvalerate; 2KIC, α-ketoisocaproate; Orot, orotate; MMA, methylmalonate; MC, methylcitrate; 3HPA, 3-OH-pyruvate; PG, propionylglycine; IVG, isovalerylglycine; MCG, methylcrotonylglycine; 3HiVA, 3-OH-isovalerate; HMGA, 3-OH-3-methylglutarate, MGA, methylglutarate; MGCA, methylglutaconate; GA, glutarate; 3HGA, 3-OH-glutarate; 2M3HBA, 2-methyl-3-OH-butyrate; TG, tiglylglycine; HG, hexanoylglycine; SG, suberylglycine; DIC, dicarboxylate; 3HDIC-3-OH-dicarboxylate; EMA, ethylmalonate.

し，考えられる診断名をアウトプットできる。このため，代謝異常症やGC/MSデータに知識のない人でも短期間のうちに使えるようになる。**Fig. 4**に自動解析結果を例示している。これによると異常として検出した代謝産物に3-OH-propionate，propionylglycinem，およびmethylcitrateがあるので，下の段に「疑わしい疾患」としてプロピオン酸血症をあげている。患者の臨床経過やタンデムマスデータなどを総合すれば，プロピオン酸血症という最終診断に比較的容易に到達することができる。

VI. タンデムマスによるアシルカルニチン分析

血液ろ紙や血清10μL程度の微量検体で，約2分間の分析時間のあいだに，アミノ酸とアシルカルニチンを分析し，そして**Fig. 5**に示すような，アシルカルニチンとアミノ酸のデータを得ることができる。アシルカルニチンはアシル基の炭素数に対応して，C2，C3，C4……と表示がされる。またアシル基に水酸基がついていればC5-OHのように表示され，不飽和結合をもつアシル基ならばC5:1，ジカルボキシル基であればC5-DCのように表現される。一方，

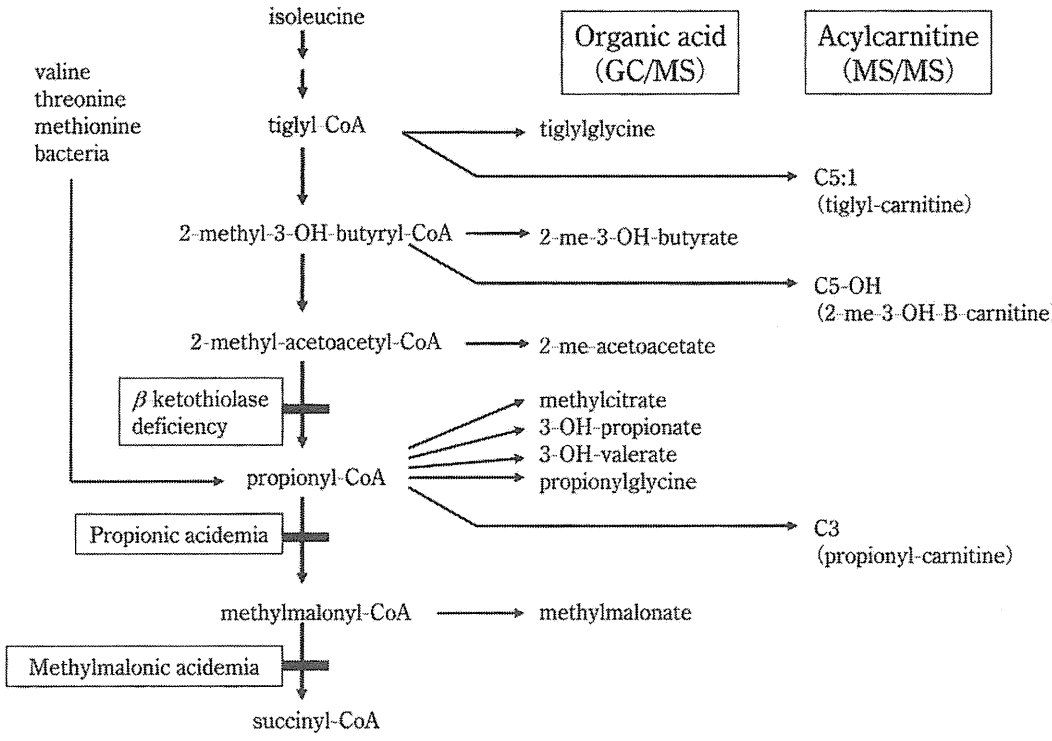

Figure 2 Metabolic pathways of isoleucine and related organic acidemia.

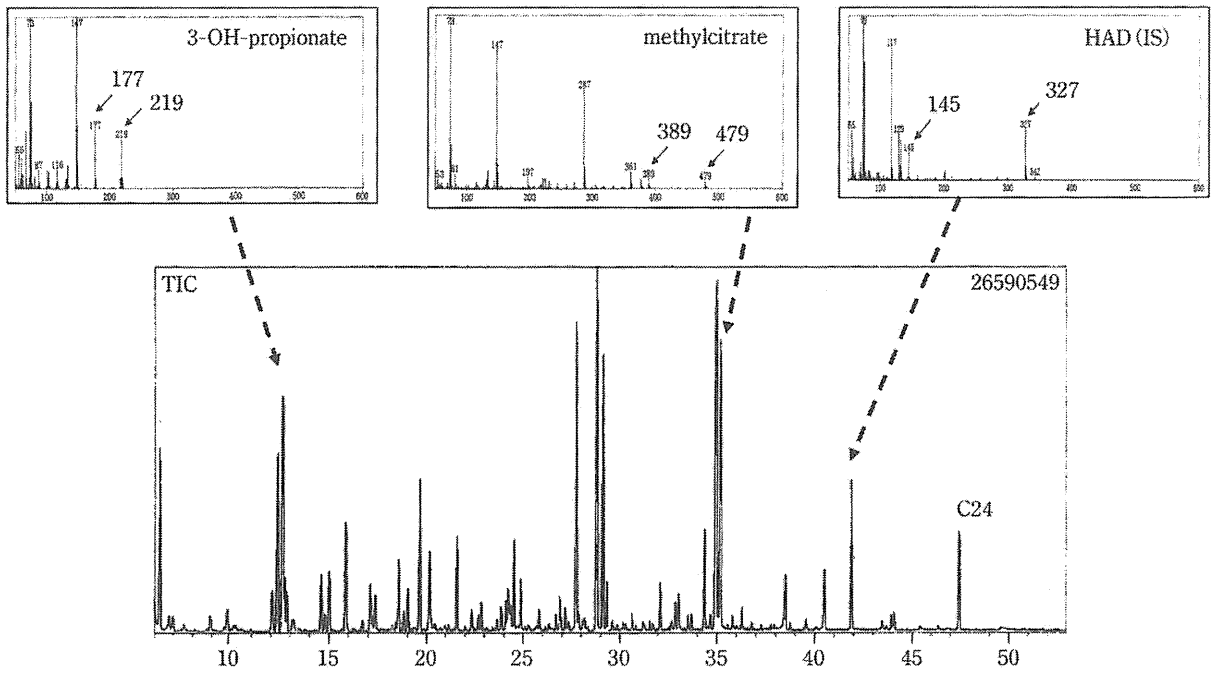

Figure 3 Gas chromatograms of urinary organic acids and mass spectrum of some peaks in propionic acidemia.
HDA, and C24 are heptadecanoate and tetracosane added internal standard.

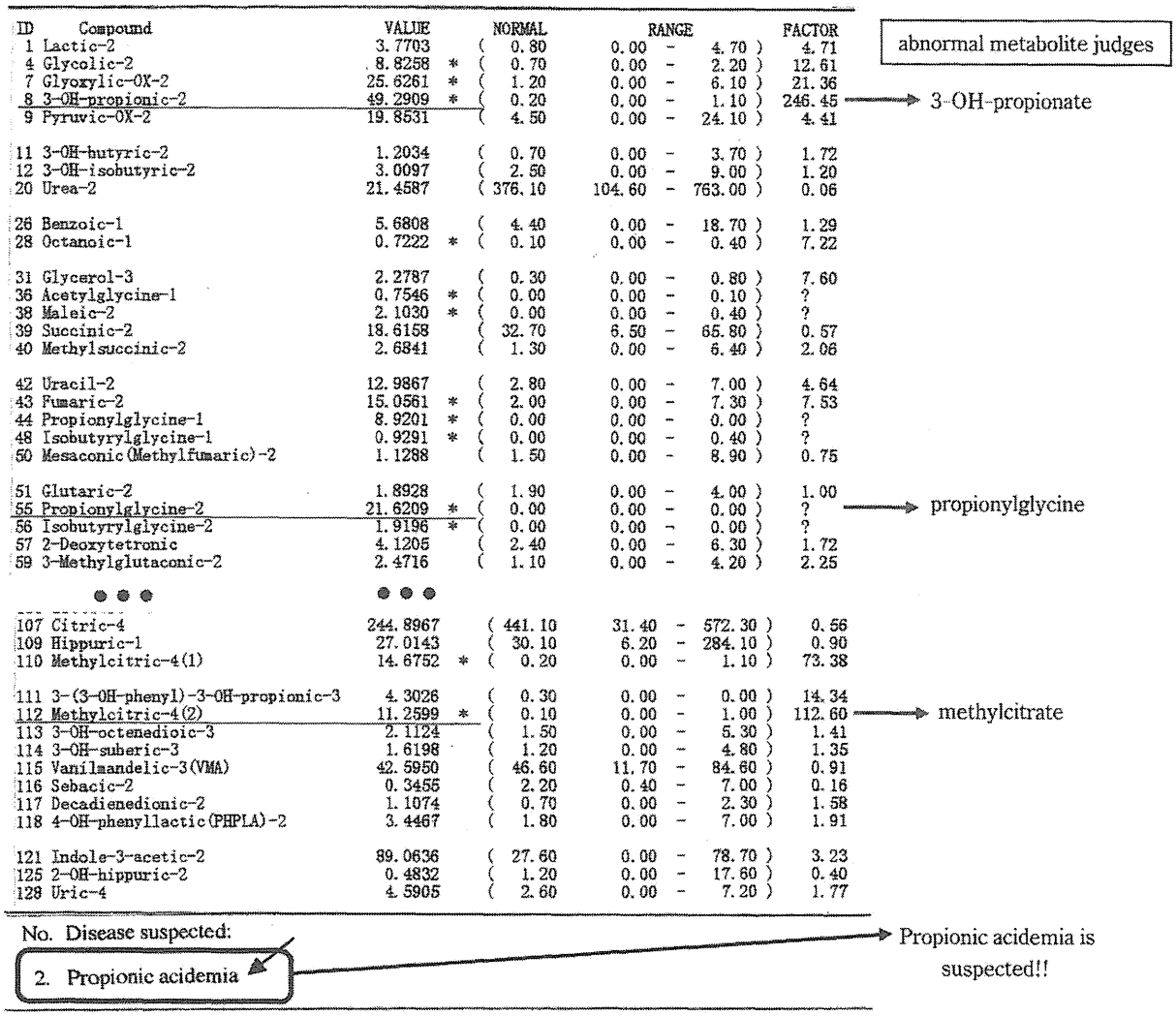

Figure 4 Results from the automated system of GC/MS data processing and autodiagnosis of propionic acidemia
*: abnormal metabolites flagged.

アミノ酸は，Phe，Tyr，Met，Leu，Val などのように表示される。

アシルカルニチンやアミノ酸の全体のプロフィールを見る方法を「スキャン法」というが，最初から測定する目標化合物を決めて，その化合物に対応するイオン質量数を設定して分析する方法を MRM 法という。MRM 法はスキャン法に比べて測定感度が数十倍に上がるが，全体のプロフィールを見ることはできなくなる。血液ろ紙を使用する新生児マススクリーニングでは，感度を上げるため MRM 分析の方がポピュラーになっている[2]。

VII. 後天性代謝異常症の診断

小児救急の場で急性脳症などに遭遇すると背景疾患のスクリーニングのために，タンデムマス分析や GC/MS 分析がポピュラーになりつつある。先天代謝異常の診断のみならず，後天性代謝障害を評価することもできる。例えば，ケトン性ジカルボン酸尿症は非常に強いケトーシスによって β 酸化が抑制されていることを表わし，非ケトン性ジカルボン酸尿症では，何らかの要因で β 酸化が抑制されていることが推測される。この他，食事性のビオチン欠乏やビタミン B12 欠乏，あるいは，チアミン欠乏による高乳酸血症，あるいは肝障害に伴うチロシン代謝の

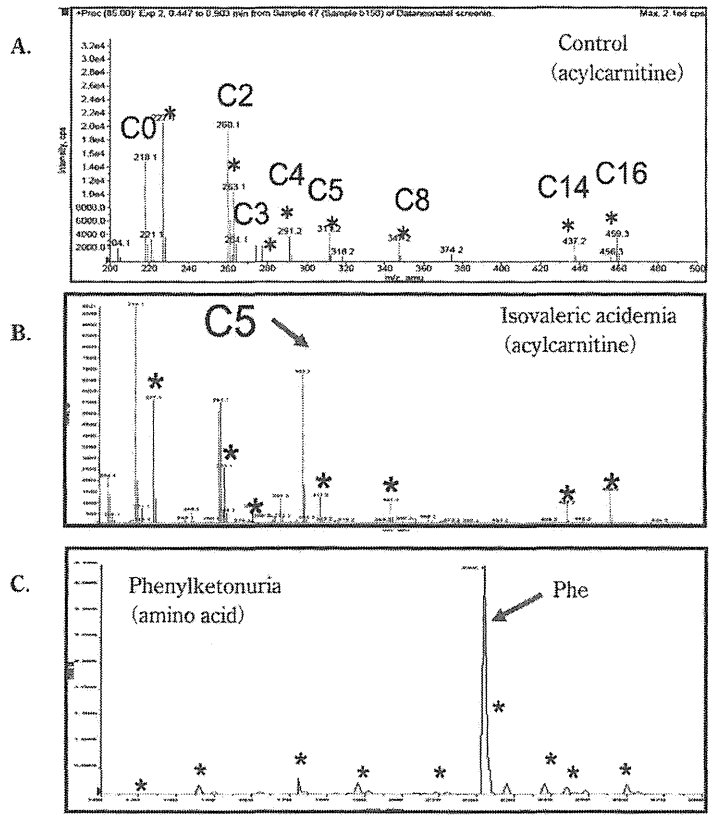

Figure 5　Mass spectrum of acylcarnitine and amino acid in MS/MS analysis (scan mode).
A, B: blood acylcarnitine analysis using MS/MS of control and isovaleric acidemia, respectively.　**C:** blood amino acid analysis using MS/MS of phenylketonuria.

障害なども生化学診断できるようになった[8]。小児救急の場にも必須の検査項目になりつつある。

VIII. おわりに

タンデムマスの新生児マススクリーニングへの導入に伴って，GC/MS による有機酸代謝異常症の診断も必須となりつつある。内科領域でも質量分析による網羅的代謝病態の評価を通じて，治療向上にも貢献することが期待される。質量分析は研究室レベルから臨床検査室へ応用が拡大しつつある。

文　献

1) 山口清次(編). 有機酸代謝異常ガイドブック. 東京: 診断と治療社; 2011.
2) 山口清次(編). タンデムマス・スクリーニングガイドブック. 東京: 診断と治療社; 2013.
3) 山口清次. 有機酸・脂肪酸代謝異常研究の進歩. 日本先天代謝異常学会誌 2005; 21: 26-36.
4) 重松陽介，布瀬光子，畑　郁江，他. Electrospray tandem mass spectrometry による有機酸およびアミノ酸代謝異常症の新生児マススクリーニング. 日本マス・スクリーニング学会誌 1998; 8: 13-20.
5) Shigematsu Y, Hirano S, Hata I, et al. Newborn mass screening and selective screening using electrospray tandem mass spectrometry in Japan. J Chromat B 2002; 776: 39-48.
6) Yamaguchi S, Iga M, Kimura M, et al. Urinary organic acids in peroxisomal disorders: a simple screening method. J Chromatogr B Biomed Sci Appl 2001; 758: 81-6.
7) Kimura M, Yamamoto T, Yamaguchi S. Automated metabolic profiling and interpretation of GC/MS data for organic acidemia screening: a personal computer-based system. Tohoku J exp Med 1999; 188: 317-34.
8) 山口清次，長谷川有紀，虫本雄一，他. GC/MS 有機酸分析で発見される小児の後天性ビタミン欠乏症: ビタミン B1 欠乏症とビオチン欠乏症. ビタミン 2012; 86: 32-6.

Hum Genet (2014) 133:225–234
DOI 10.1007/s00439-013-1372-6

ORIGINAL INVESTIGATION

A hemizygous *GYG2* mutation and Leigh syndrome: a possible link?

Eri Imagawa · Hitoshi Osaka · Akio Yamashita · Masaaki Shiina · Eihiko Takahashi · Hideo Sugie · Mitsuko Nakashima · Yoshinori Tsurusaki · Hirotomo Saitsu · Kazuhiro Ogata · Naomichi Matsumoto · Noriko Miyake

Received: 17 April 2013 / Accepted: 29 September 2013 / Published online: 8 October 2013

Abstract Leigh syndrome (LS) is an early-onset progressive neurodegenerative disorder characterized by unique, bilateral neuropathological findings in brainstem, basal ganglia, cerebellum and spinal cord. LS is genetically heterogeneous, with the majority of the causative genes affecting mitochondrial malfunction, and many cases still remain unsolved. Here, we report male sibs affected with LS showing ketonemia, but no marked elevation of lactate and pyruvate. To identify their genetic cause, we performed whole exome sequencing. Candidate variants were narrowed down based on autosomal recessive and X-linked recessive models. Only one hemizygous missense mutation (c.665G>C, p.W222S) in glycogenin-2 (*GYG2*) (isoform a: NM_001079855) in both affected sibs and a heterozygous change in their mother were identified, being consistent with the X-linked recessive trait. *GYG2* encodes glycogenin-2 (GYG2) protein, which plays an important role in the initiation of glycogen synthesis. Based on the structural modeling, the mutation can destabilize the structure and result in protein malfunctioning. Furthermore, in vitro experiments showed mutant GYG2 was unable to undergo the self-glucosylation, which is observed in wild-type GYG2. This is the first report of *GYG2* mutation in human, implying a possible link between GYG2 abnormality and LS.

Introduction

Glycogen is a large branched polysaccharide containing linear chains of glucose residues. Glycogen deposits in skeletal muscle and liver serve as shorter-term energy storage in mammals, while fat provides long-term storage. Glycogen biosynthesis begins with self-glucosylation of glycogenins by covalent binding of UDP-glucose to tyrosine residues of the glycogenins and the subsequent extension of approximately ten glucose residues (Pitcher et al. 1988; Smythe et al. 1988). Glycogen particles are formed by the continued addition of UDP-glucose to the growing

Electronic supplementary material The online version of this article (doi:10.1007/s00439-013-1372-6) contains supplementary material, which is available to authorized users.

E. Imagawa · M. Nakashima · Y. Tsurusaki · H. Saitsu · N. Matsumoto (✉) · N. Miyake (✉)
Department of Human Genetics, Yokohama City University Graduate School of Medicine, Yokohama 236-0004, Japan
e-mail: naomat@yokohama-cu.ac.jp

N. Miyake
e-mail: nmiyake@yokohama-cu.ac.jp

H. Osaka
Division of Neurology, Clinical Research Institute, Kanagawa Children's Medical Center, Yokohama 232-8555, Japan

A. Yamashita
Department of Molecular Biology, Yokohama City University School of Medicine, Yokohama 236-0004, Japan

M. Shiina · K. Ogata
Department of Biochemistry, Yokohama City University Graduate School of Medicine, Yokohama 236-0004, Japan

E. Takahashi
Division of Infection and Immunology, Clinical Research Institute, Kanagawa Children's Medical Center, Yokohama 232-8555, Japan

H. Sugie
Department of Pediatrics, Jichi Medical University, Tochigi 329-0498, Japan

glycogen chain by glycogen synthase, and introduction of branches every 10–14 residues by the glycogen branching enzyme (Krisman and Barengo 1975; Larner 1953). To date, two glycogenin paralogues have been identified in human, glycogenin-1 (GYG1) and glycogenin-2 (GYG2). These proteins have been shown to form homodimers, heterodimers and larger oligomers (Gibbons et al. 2002). GYG1 (muscle form) is expressed predominantly in muscle while GYG2 (liver form) is expressed mainly in liver, heart and pancreas (Barbetti et al. 1996; Mu et al. 1997). Biallelic GYG1 abnormality is known to cause muscle weakness and cardiac arrhythmia in humans through GYG1 autoglucosylation failure (Moslemi et al. 2010). However, human disease due to GYG2 abnormality has never been reported.

Leigh syndrome (LS; MIM #256000) was first described as a subacute necrotizing encephalomyelopathy by Dr. Denis Leigh in 1951 (Leigh 1951). LS is a progressive neurodegenerative disorder with an estimated incidence of 1:40,000 live births (Rahman et al. 1996). Onset is usually in early childhood (typically before age 2) (Naess et al. 2009; Ostergaard et al. 2007). Clinical manifestations of LS are observed in the central nervous system (CNS) (developmental delay, hypotonia, ataxia, convulsion, nystagmus, respiratory failure and dysphagia), peripheral nervous system (polyneuropathy and myopathy) and extraneural organs (deafness, diabetes, cardiomyopathy, kidney malfunction and others) (Finsterer 2008). The neurological features depend on the affected regions and degree of severity. The presence of bilateral, symmetrical, focal hyperintense T2-weighted MRI signals in basal ganglia (mainly putamen), thalamus, substantia nigra, substantia ruber, brainstem, cerebellum, cerebral white matter or spinal cord is diagnostic of LS (Farina et al. 2002; Medina et al. 1990). Neuropathological studies revealed that these lesions reflect neuronal necrosis, gliosis and vascular proliferation (Brown and Squier 1996; Leigh 1951). In the majority of LS cases, lactate, pyruvate or the lactate/pyruvate ratio is increased in blood and cerebrospinal fluid (Finsterer 2008). To the best of our knowledge, 37 nuclear genes are known to be mutated in LS, in addition to some mitochondrial genes (Antonicka et al. 2010; Debray et al. 2011; Finsterer 2008; Lopez et al. 2006; Martin et al. 2005; Quinonez et al. 2013). Thus, inheritance patterns of LS include mitochondrial, autosomal recessive and X-linked recessive modes (Benke et al. 1982; van Erven et al. 1987).

We encountered a Japanese family with affected brothers showing atypical LS without marked elevation of lactic or pyruvic acid and unknown etiology. A unique genetic variant was identified by whole exome sequencing (WES), which may be associated with atypical LS phenotype in this family.

Materials and methods

Subjects

Peripheral blood samples of affected brothers diagnosed with LS and their parents were collected after obtaining written informed consent. DNA was extracted from peripheral blood leukocytes using QuickGene-610L (Fujifilm, Tokyo, Japan) according to the manufacturer's instructions. Lymphoblastoid cell lines derived from all family members were established. The Institutional Review Boards of Yokohama City University School of Medicine approved this study.

Causative gene identification

Whole exome sequencing was performed in two affected individuals (II-2 and II-3 in Fig. 1a) as described in the Supplementary methods. All candidate variants based on autosomal and X-linked recessive models were checked by Sanger sequencing in the parents and affected siblings. PCR products amplified with genomic DNA as a template were sequenced on an ABI3500xl autosequencer (Applied Biosystems, Foster City, CA) and analyzed using Sequencher 5.0 (Gene Codes Corporation, Ann Arbor, MI). As the pedigree tree might also indicate mitochondrial inheritance of this disease and LS is known to be caused by mitochondrial genome mutations, we screened the entire mitochondrial genome by the algorithm reported previously (Picardi and Pesole 2012), using exome data (detailed in Supplementary methods).

Structure modeling

To evaluate the effect of the GYG2 missense mutation (c.665G>C, p.W222S in isoform a: NM_001079855) on its function at the molecular structural level, the mutated molecular structure was constructed, and the free energy change caused by the mutation was calculated using the FoldX software (version 3.0) (Guerois et al. 2002; Khan and Vihinen 2010). As crystal structure of human GYG2 is unavailable, that of human GYG1 (Protein Data Bank code; 3T7O) was used as a structural model. The mutation was introduced into one subunit of the GYG1 homodimer. The ligands included in the crystal structure of GYG1 were ignored in the calculation, because the FoldX energy function could not deal with the ligands. The calculation was repeated three times, and the resultant data were presented as an average value with standard deviations.

Preparation for mammalian expression vectors

Human glycogenin-2 isoform a cDNA clone (IMAGE Clone ID: 100008747) integrated in pENTR221 was purchased from Kazusa DNA Research Institute (Chiba, Japan). The

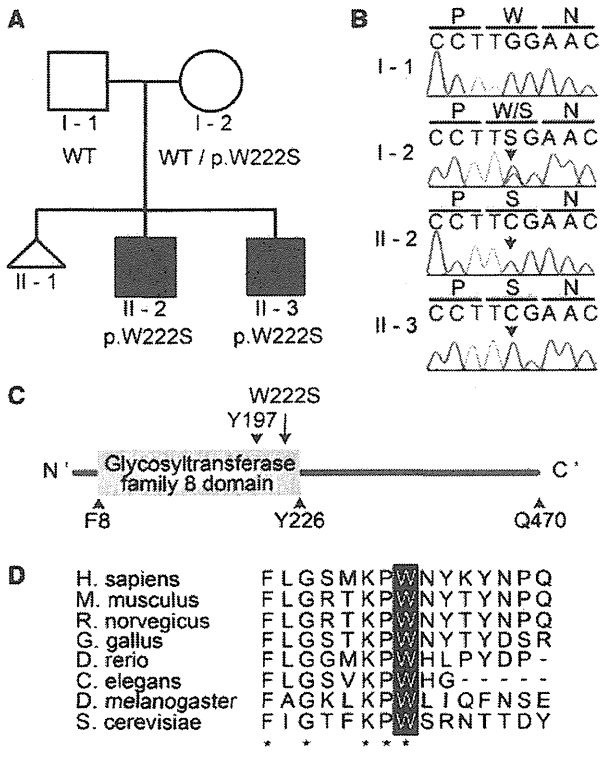

Fig. 1 Mutation Analysis of *GYG2*. **a** Pedigree of the family with a unique type of LS and a *GYG2* mutation (c.665G>C, p.W222S). *Square*, *circle* and *triangle* denote male, female and spontaneous abortion, respectively. *White* and *black symbols* indicate unaffected and affected individuals, respectively, while the affection status of the spontaneous abortion is unknown. **b** Electropherograms of a *GYG2* mutation. **c** The functional domain of human GYG2 (isoform a). The substitution of p.W222S is located within the glycosyltransferase family 8 domain (*yellow square*). **d** The evolutionary conservation of the W222 in GYG2. *Red stars* indicate identical amino acids from *S. cerevisiae* to *H. sapiens*. Sequences were aligned using CLUSTALW (http://www.genome.jp/tools/clustalw/)

missense mutation (c.665G>C, p.W222S) was introduced by Site-directed mutagenesis using the QuikChange II XL site-directed mutagenesis kit (Agilent Technologies, Santa Clara, CA). Wild-type and mutant C' V5/6xHis tagged GYG2 constructs were created using pcDNA-DEST40 (Invitrogen, Carlsbad, CA) by LR recombination in Gateway system (Invitrogen). To create the untagged construct, the last codon was altered to a stop codon by mutagenesis.

Self-glucosylation analysis

Glucosyltransferase activity of GYG2 was measured as previously described (Lomako et al. 1988), with slight modifications. In brief, COS-1 cells were maintained in Dulbecco's modified Eagle's medium (DMEM) (Sigma-Aldrich, Schnelldorf, Germany) containing 10 % heat-inactivated fetal bovine serum (FBS) (Gibco-BRL, Grand Island, NY), 2 mM L-glutamine (Sigma-Aldrich) and 1 % penicillin–streptomycin (Sigma-Aldrich). As previously described (Mu and Roach 1998), the ~80 % confluent COS-1 cells (~1 × 10^7) were transiently transfected by X-treamGENE9 DNA transfection reagent (Roche Applied Science, Foster City, CA) with 5 μg of either a wild-type Human GYG2 (isoform a) expressing plasmid or the same plasmid into which the W222S encoding mutation had been introduced. After 24 h, the cells were collected and lysed in 300 μl of buffer consisting of 50 mM HEPES, 0.5 % Triton X-100, 1 × EDTA-free protease Inhibitor Cocktail tablets (Roche Applied Science), 1 × phosphatase inhibitor cocktail (Nacalai Tesque Inc., Kyoto, Japan) and 0.5 mM β-mercaptoethanol (Mu et al. 1997). After centrifugation at 14,000 rpm for 15 min, 10 μl of the soluble fractions were mixed with 10 μl of 2 × reaction buffer containing 100 mM HEPES (pH7.5), 10 mM MgCl, 4 mM dithiothreitol (DTT) and 40 μM UDP-[^{14}C]-glucose (250 mCi/mmol; PerkinElmer, Waltham, MA) (Cao et al. 1993). After incubation at 30 °C for 30 min, the reaction was stopped by addition of 20 μl of 2 × Laemmli sample buffer (Sigma-Aldrich) (Viskupic et al. 1992). 15 μl of each sample was subjected to SDS-polyacrylamide gel electrophoresis. After treatment with Gel drying solution (Bio-Rad Laboratories, Hercules, CA) for 30 min, gels were dried. Dried gels were then exposed on X-ray film for 2 weeks to detect the incorporation of UDP-[^{14}C]-glucose into GYG2. In addition, the ^{14}C-signal intensities were evaluated using an imaging analyzer, BAS2500 (Fujifilm). Three independent experiments were performed.

Western blot analysis

For the detection of GYG2 protein, rabbit polyclonal anti-GYG2 antibodies (1:500 dilution; Abcam Inc., Cat.#HPA005495, Cambridge, MA) and horse-radish peroxidase (HRP)-conjugated anti-rabbit IgG (1:10,000 dilution; Jackson ImmunoResearch, Cat.#111-035-003, West Grove, PA) were used. Immunoblot chemiluminescence was performed using SuperSignal West Dura as substrate (Thermo Fisher Scientific, Waltham, MA). The chemiluminescence signal images were captured by FluorChem 8900 (Alpha Innotech, San Leandro, CA). Signal intensities were measured by AlphaEase FC (Alpha Innotech). Three independent experiments were performed.

Results

Clinical finding

Patient II-2 (Fig. 1a; Table 1) is a 26-year-old male born to non-consanguineous parents. His mother previously had a

Table 1 Clinical features of the presenting patients affected with LS

	II-2	II-3
Sex	M	M
Age (years)	26	19
Common clinical phenotype		
Psychomotor retardation	+	+
Failure to thrive	+	+
Swallowing difficulties	–	–
Spasticity	+	+
Rigidity	+	+
Pathological reflexes	+	+
Ataxia	+	+
Athetoid movements	+	+
Convulsions	+	+
Ophthalmoplegia	+	+
Strabismus	+	+
Gastrointestinal problems	+	+
Renal agenesis	NA	+
Pes equinovarus	+	+
Uncommon clinical phenotype		
Increase of ketone body	+	+

NA not assessed

spontaneous abortion. He was born at 39 weeks gestation without asphyxia after an uneventful pregnancy. His body weight was 3,680 g (+1.6 SD), his height was 50.0 cm (−0.5 SD), and his head circumference (HC) was 34.0 cm (−0.5 SD). His early developmental milestones were normal with head control and reach to toys at 4 months, roll at 6 months and grasp with two fingers at 7 months. At 10 months, he was referred to our hospital because of an inability to sit. His body weight was 9,120 g (±0.0 SD), his height was 76.0 cm (+1.3 SD), and his HC was 48.0 cm (+1.4 SD). He could smile and swallow well. Bilateral strabismus was noted. No minor anomalies were noticed. Muscle tone was normal. Deep tendon reflexes were normal with negative Babinski sign. He showed athetoid movements of trunk and extremities. He showed pes equinovarus at traction response. Levels of lactate and pyruvate were normal with 12.2 and 0.89 mg/dl (L/P ratio = 13.7), respectively. Other laboratory examinations, including blood gas, blood sugar, ammonia, AST, ALT, BUN, Creatine, TSH, T3, T4, amino acids, and urine organic acid analyses were all normal. Electroencephalogram (EEG) showed no abnormalities. He was suspected to have dyskinetic cerebral palsy and referred to the division of rehabilitation. He could crawl at the age of 2. At 6 years, he experienced a loss of consciousness followed by generalized tonic–clonic convulsion with fever and was admitted to another hospital. He was diagnosed with bilateral infarction of the basal ganglia. Although EEG showed no abnormalities, clonazepam was started with the suspicion of symptomatic epilepsy. At the age of 9, he was referred to us again. His weight was 19.1 kg (−4.5 SD), his height was 115.0 cm (−2.8 SD). He lost the ability to speak several words and switched handedness from right to left. He also showed other signs of regression: including spasticity with elevated deep tendon reflexes and positive Babinski sign. In addition, he suffered bilateral hip joint dislocations and the foot deformity became worse. Contractures were noted in all extremities. Brain magnetic resonance imaging (MRI) revealed a bilateral necrotic lesion of the globus pallidus (Fig. 2a, b). EEG and motor conduction velocities were normal. Laboratory examinations, including lactate and pyruvate, were all normal. At the age of 12, he was admitted with acute bronchitis, at that time he showed an increase of blood ketone bodies: acetoacetic acid, 720 μmol/l; 3OHBA, 974 μmol/l and urine ketone (+++). Blood levels of ammonia (18 μmol/l), sugar (125 mg/dl) and lactate/pyruvate (5.1/0.29 mg/dl) were all within normal range. The values of blood ketone bodies returned to normal level with the cease of fever. Deficiencies of 3-ketothiolase and succinyl-CoA:3-oxoacid CoA transferase were ruled out by enzyme analysis using fibroblasts. His clinical symptoms and repeated MRI show the non-progressive course of his disease. Currently he is unable to sit or speak any words. Despite the addition of carbamazepine and lamotrigine, he still exhibits generalized tonic–clonic convulsion a few times a year. He also takes medicine for hypertonicity including dantrolene sodium, diazepam, baclofen and levodopa.

Patient II-3 (Fig. 1a; Table 1), the younger brother of II-2, was born uneventfully. He was born at 37 week's gestation without asphyxia after an uneventful pregnancy. His body weight was 3,668 g (+1.5 SD), his height was 50.0 cm (+0.5 SD), and his HC was 36.0 cm (−0.5 SD). He suffered from bacterial meningitis of unknown origin at 1 month of age. He became unconscious followed by convulsion and gastroenteritis at 1 year and 11 months. Brain MRI showed marked swelling of the basal ganglia (Fig. 2c, d). He was diagnosed with bilateral infarction of the basal ganglia. After this event, he became left handed. When he was 2 years old, surgery was performed to correct bilateral inner strabismus. He was referred to our hospital at the age of 4 for evaluation. His body weight was 11.0 kg (−2.2 SD), his height was 92.5 cm (−1.2 SD), and his HC was 49.5 cm (−1.3 SD). He could respond with a smile to his mother's voice. Motor milestones were delayed with no head control. No minor anomalies were noticed. Muscle tone was hypotonic. Deep tendon reflexes were exaggerated with positive Babinski sign and ankle clonus. He showed pes equinovarus. He showed a significant increase of blood acetoacetic acid of 1,270 μmol/l and 3-OHBA of 3,270 μmol/l. Levels of blood lactate and pyruvate were normal (6.2 and 0.48 mg/dl, respectively, L/P ratio = 12.9).

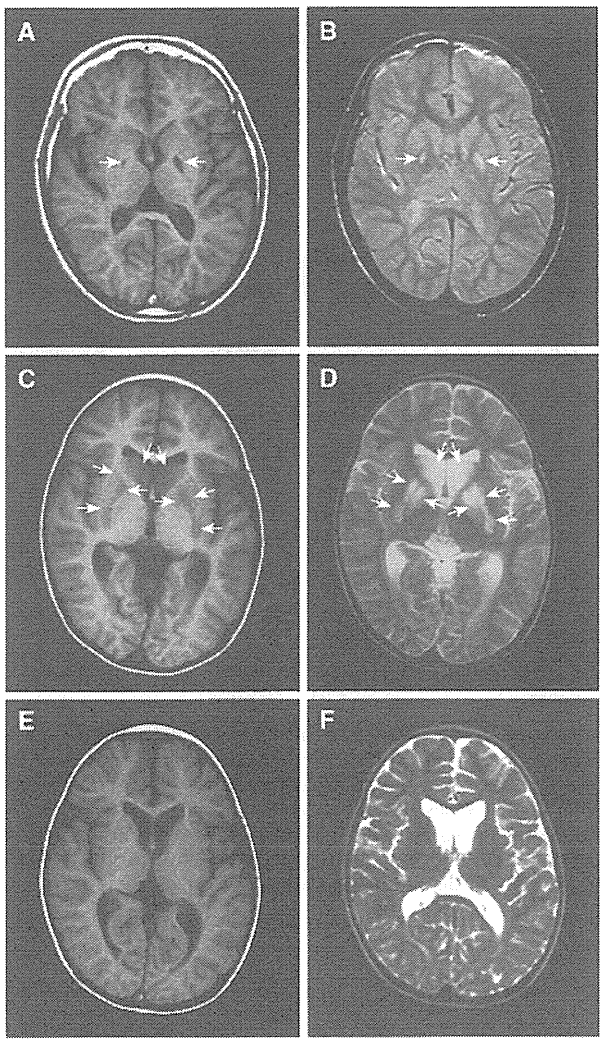

Fig. 2 Brain MRI of affected patients with a *GYG2* mutation. **a**, **b** (Patient II-2): T1 (**a**) and T2 (**b**) weighted brain magnetic resonance imaging (MRI) show necrotic lesion of bilateral globus pallidus (*arrows*). T2 elongation is observed at deep white matter at 1 year. **c–f** (Patient II-3): MRI at 1 year and 11 months shows swellings of caudate nuclei, globus pallidus, and putamen with the decreased T1 intensity (**c**) and increased T2 signals (**d**). *Arrows* indicate swollen lesions in basal ganglia. At 4 years (**e**, **f**), swelling of basal ganglia disappeared with continued mild high intensity in T2 weighted image (**f**)

Lactate and pyruvate levels of cerebrospinal fluid were slightly elevated with 11.3 and 1.11 mg/dl, respectively. Other laboratory examinations, including blood gas, blood sugar, ammonia, AST, ALT, BUN, Creatine, TSH, T3, T4, amino acids, and lysosomal enzymes were all normal. Urine organic acid analyses showed an increase of acetoacetic acid, 3-OHBA, and 3-OH-isovaleric acid. EEG showed no paroxysmal discharges. Muscle biopsy showed no specific abnormalities and no ragged red fibers. Staining for cytochrome c oxidase was normal (data not shown). Brain MRI disclosed T2 elongation in the basal ganglia and cerebral deep white matter (Fig. 2e, f). At the age of 5, he showed lethargy with fever. At 6 years, he again showed lethargy. Biochemical analysis disclosed a significant increase of blood ketone bodies: acetoacetic acid, 1,337 μmol/l; 3-OHBA, 4,845 μmol/l and urine ketone (+++). Blood levels of ammonia (28 μmol/l), sugar (78 mg/dl), lactate (5.1 mg/dl) and pyruvate (0.43 mg/dl) were all within normal range. Blood gas analysis revealed metabolic ketoacidosis with an increase of anion gap; 22.4 mEq/l (normal range 12 ± 2). His consciousness and biochemical measurements returned to normal within a few days with intravenous fluid infusion. Similar ketoacidosis attacks were repeatedly observed and agenesis of the left kidney and neurogenic bladder were recognized at the age of 8. He started intermittent urinary catheterization, and suffered from repeated urinary tract infections, resulted in chronic renal failure. Repeated brain MRI shows the progression of cerebral and cerebellar atrophy. He is now 19 years old and shows no gain of motor or intellectual abilities from the age of 4. He takes dantrolene sodium and diazepam for hypertonicity, and spherical charcoal, allopurinol for renal failure.

Identification of a *GYG2* variant by exome sequencing

A total of 2,433,011,483 bps (II-2) and 7,926,169,749 bps (II-3) were mapped to RefSeq coding DNA sequence (CDS). 83.3 and 96.0 % of CDS were covered by ten reads and more. We used only NGS data of II-3 for selecting candidate variants as the lower-quality NGS data of II-2 may lead to erroneous conclusion. Based on the hypothesis that this syndrome is inherited in an autosomal recessive or an X-linked recessive fashion, we focused on homozygous or compound heterozygous variants on autosomes and hemizygous variants on the X chromosome. While nine variants in four candidate genes were selected by in silico flow, only one hemizygous missense mutation in *GYG2* gene agreed with the familial segregation pattern (autosomal recessive or X-linked recessive) (Table S1, S2). The c.665G>C (p.W222S) in *GYG2* (isoform a: NM_001079855) was hemizygous in affected sibs and heterozygous in their mother, consistent with the X-linked recessive model, and was confirmed by Sanger sequence (Fig. 1b). The variant was absent in our in-house Japanese exome data ($n = 418$), the 1,000 Genomes database and ESP6500. Furthermore, no pathological variants in mtDNA were detected by exome sequence (Supplementary Results, Figure S1). In addition, a total of 21 LS patients (12 males and 9 females) were screened, but no pathological changes were found in *GYG2*.

GYG2 encodes GYG2 proteins with at least five isoforms: isoform a (NM_001079855), isoform b (NM_003918),

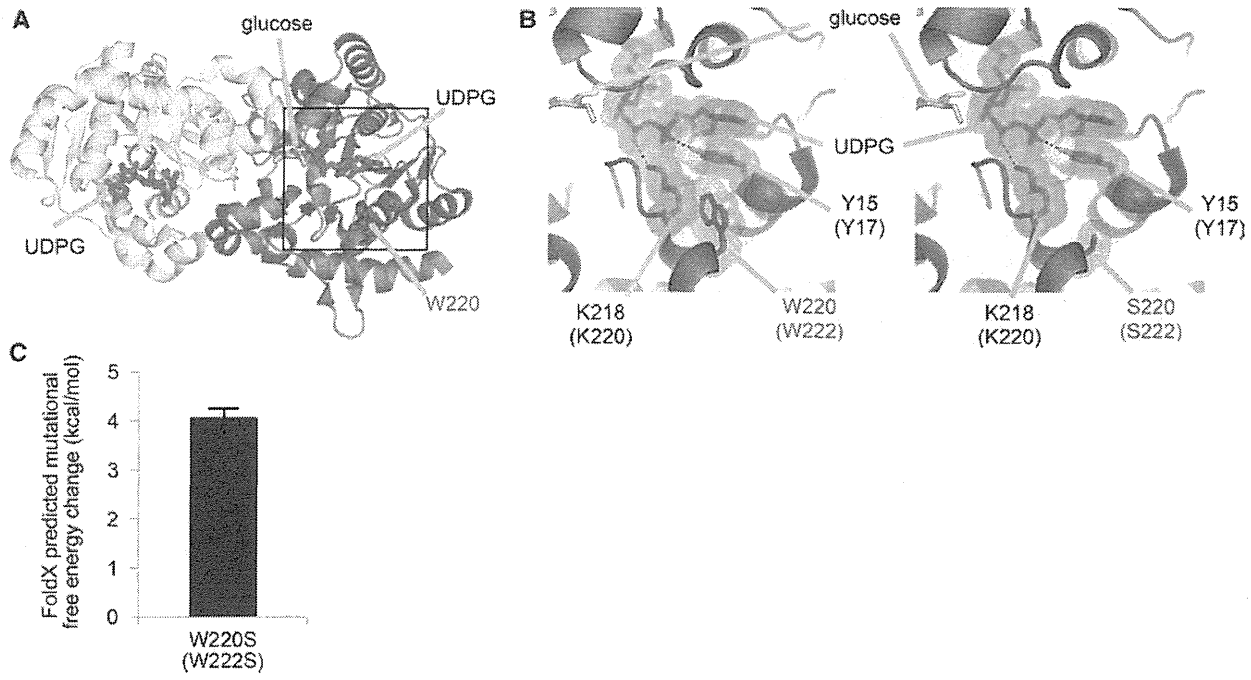

Fig. 3 Molecular structural consideration of the W222S mutation of GYG2. **a** Crystal structure of human GYG1 (Protein Data Bank code; 3T7O) (Chaikuad et al. 2011). Each monomer is colored *yellow* and *cyan*. α-helices, β-sheet and loops are drawn as *ribbons*, *arrows* and *threads*, respectively. The side chain of W222, glucose and UDP-glucose (UDPG) are shown as *sticks* in *red*, *orange* and *green*, respectively. Amino acid numbering shown is for human GYG1 with that for human GYG2 in *parenthesis*. The *squared area* corresponds to the close-up views in (**b**). **b** Detailed views of structures of the wild-type (*left*) and mutated GYG2 (p.W222S) (*right*). Amino acid residues at positions of 15, 218 and 220 and UDPG are shown as sticks with van der Waals representation and annotations. Hydrogen bonds are depicted as *dotted lines*. **c** Calculated free energy change upon the p.W222S mutation of GYG2 using FoldX software. All the molecular structures were drawn using PyMOL (www.pymol.org)

isoform c (NM_001184702), isoform d (NM_001184703), and isoform e (NM_001184704). At least two GYG2 isoforms (isoform a and b) are expressed preferentially in liver, heart and pancreas (Mu et al. 1997), while the detailed expression and function of other isoforms are undetermined. GYG2 has a glycosyltransferase family 8 domain and initiates glucose addition on its Tyrosine residue (Y197 in isoform a) via *O*-glycosylation (self-glucosylation) and can also attach an additional 7–10 residues of UDP-glucose to itself (Bollen et al. 1998; Lomako et al. 2004; Zhai et al. 2001). The W222 within the glycosyltransferase family 8 domain is evolutionarily highly conserved from *S. cerevisiae* to *H. sapiens* (Fig. 1c, d). In addition, all isoforms contain this residue. Thus, it is thought that this mutation may impair its biological function.

Structural consideration of the p.W222S mutation in human GYG2

The amino acid residue W222 of GYG2 (isoform a) was mapped to the crystal structure of human GYG1 (Chaikuad et al. 2011), since no experimental structure of GYG2 was available. W222 is involved in a hydrophobic core near the UDP-glucose (UDPG) binding site along with Y17 and K220 (Fig. 3a, b). The side chains of Y17 and K220 are hydrogen-bonded to UDPG, and the former also makes van der Waals contacts with the uridine ring of UDPG in a stacking mode. Therefore, the formation of the hydrophobic core appears to be a prerequisite for UDPG binding. To estimate the impact of the W222S mutation on the protein stability, we modeled the mutant structure and calculated the free energy change upon the mutation using the FoldX software. As a result, the mutation was predicted to destabilize the protein structure with about 4 kcal/mol increase in free energy (Fig. 3c). This suggests that the W222S mutation would impair UDPG binding (Fig. 3b).

Self-glucosylation analysis

To see the functional effects of the *GYG2* mutation in vitro, glucosyltransferase activity monitoring by self-glucosylation was measured using wild-type (WT) and W222S mutant (Mut) GYG2 (isoform a) transiently

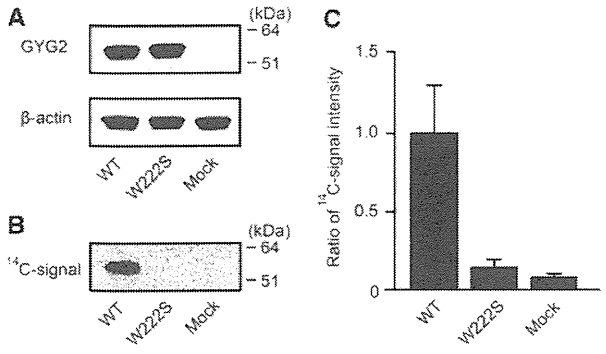

Fig. 4 Enzyme activity of GYG2. **a** Western blot analysis of recombinant GYG2. Wild-type (WT) and mutant (p.W222S) GYG2 was detected at the expected size (52 kDa). β-actin (42 kDa) was used as an internal control. **b** Autoradiography images presenting ^{14}C glucosylation toward GYG2. The signal was detected in WT, but undetected in mutant, with similar levels to Mock. **c** Graphic presentation of autoglucosylation of GYG2. The activity detected in Mock might be due to the endogenous glycogenin. *Error bars* represent the standard error of the mean

overexpressed in COS-1 cells. By immunoblotting, the expected 52 kDa bands of recombinant WT and Mut GYG2 were detected with similar expression levels (Fig. 4a). While WT GYG2 showed reasonable glucosyltransferase activity, Mut GYG2 almost completely lost the enzyme activity and was similar to the Mock level (Fig. 4b, c).

Expression analysis of GYG1 and GYG2

To observe tissue distribution of the human *GYG1* and *GYG2*, expression analysis was performed using multiple tissue cDNA panels. *GYG1* was expressed preferentially in skeletal muscle and heart from fetus to adult stages as previous reports (Barbetti et al. 1996). *GYG2* is dominantly expressed in liver from fetus through adult stages and moderately expressed in brain, heart, pancreas and kidney (Supplementary Results, Figure S2). To be marked, *GYG1* is not expressed in liver and brain where *GYG2* is highly expressed.

Discussion

In this study, we analyzed unique brothers affected with LS who were born to non-consanguineous healthy parents after uneventful pregnancies. Patient II-2 and II-3 developed LS accompanied by delayed developmental milestones at 10 months and 13 months of age, respectively. Their age of onset, clinical features and brain imaging were compatible with the diagnosis of LS. Interestingly, CNS abnormalities were observed (developmental delay, convulsion, athetoid movements, nystagmus, hypotonia, spasticity, increased deep tendon reflex and abnormal reflection), but involvement of peripheral nerve and extraneural organs was obscure. Based on the facts including (1) male (X-linked recessive), (2) normal lactate/pyruvate, (3) ketonemia/ketonuria, and (4) CNS predominant symptoms, the hemizygous *GYG2* mutation was highlighted a primary culprit.

In this study, we first identified a human *GYG2* mutation in affected brothers with LS with ketonemia/ketonuria but normal blood lactate/pyruvate. We can hypothesize a pathomechanism of the *GYG2* impairment in this family based on the canonical pathway of glycogen metabolism (Fig. 5). As glycogen storage in liver might be decreased because of the GYG2 malfunction, glucose is easily depleted. To keep appropriate blood glucose concentrations, the metabolism would be shifted toward gluconeogenesis and beta-oxidation to create glucose and energy sources like Acetyl-CoA (Garber et al. 1974; Laffel 1999; Randle et al. 1964). Excess beta-oxidation would result in overproduction of ketone bodies, consistent with the observation of ketonemia and ketonuria. However, pyruvate and lactate could be normally metabolized in gluconeogenesis and/or TCA cycle and would not accumulate in the body as seen in the majority of LS patients. Interestingly, both patients showed normal blood glucose level while showing LS manifestations which might be due to tissue energy depletion. In GYG2-deficient patients, the CNS was dominantly affected, while the effect of this abnormal metabolism was thought to extend to the entire body. This predominance could be explained by high glucose consumption as the primary energy source in brain (Amaral 2012; Magistretti and Pellerin 1999) and glycogen depletion in brain tissue level, while the blood sugar level was maintained by the other compensatory mechanism. This is similar to the muscle specific phenotypes (muscle weakness and arrhythmia) observed in patients with deficiencies of "muscle form" GYG1 in the absence of hypoglycemia (Moslemi et al. 2010). Remarkably, glycogen was less in the muscle tissue of GYG1 depleted patient (Moslemi et al. 2010). These evidences might indicate that it is not always linked between glucose level in the peripheral blood and glycogen/energy supply in tissue level while we could not show the loss of glycogen in liver or brain tissues because the materials were not available. In addition, deficiencies in two paralogous enzymes, GYG1 and GYG2, result in different human diseases suggesting they are unable to compensate each other in specific organs.

The *GYG2* mutation is probably causative for LS in this family. However, it is possible that the mutation is just coincidence because we just showed genetic evidences (due

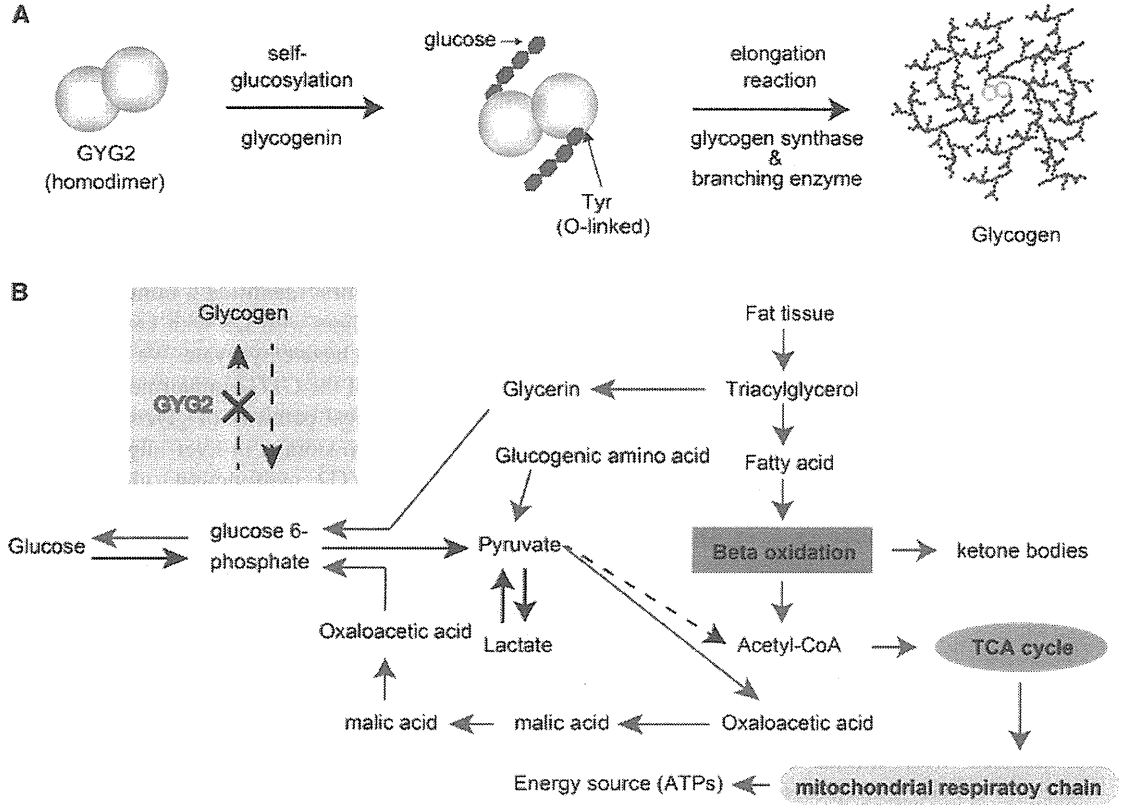

Fig. 5 Biochemical metabolisms in glycogen storage and glycolysis pathways. **a** Schematic presentation of glycogen biosynthesis. GYG2 has a catalytic capability for *O*-linked self-glucosylation at Tyrosine (Y197 in isoform a) and adds approximately 10 glucose molecules. By the subsequent elongating reactions by glycogen synthase and branching enzyme, giant molecule "glycogen" is formed. **b** Modeled biochemical pathway in GYG2 impairment. As the GYG2 impairment results in the absence of glycogen storage, glycogen is easy to be depleted and gluconeogenesis is induced from fat tissues and glucogenic amino acids. The reactions in mitochondria are shown in *yellow shadow*. While increased acetyl-CoA inhibits the pyruvate dehydrogenase complex which irreversibly converts pyruvate to acetyl-CoA (as shown as *dotted line*), it accelerates gluconeogenesis through pyruvate–oxaloacetic acid–malic acid–oxaloacetic acid. Triacylglycerol was metabolized into glycerin and fatty acid. Fatty acid was used for beta-oxidation and ketone production. The *arrows* indicate the directions of normal metabolism. *Red arrows* indicate the predicted predominant pathways in GYG2-deficient patients

to its rarity and familial co-segregation) and GYG2 loss of function by in vitro study without showing any sufficient data on how the *GYG2* mutation causes LS.

In conclusion, we describe the first human variant of *GYG2* which may be associated with the atypical LS phenotype in this family. Further studies are absolutely needed to conclude whether *GYG2* abnormality leads to atypical LS observed in this family.

Acknowledgments We thank all the patients and their families for participating in this work. We deeply appreciate Dr. Toshiyuki Fukao, who is the professor of Department of Pediatrics, Graduate School of Medicine, Gifu University, for the enzyme assay for 3-ketothiolase deficiency and succinyl-CoA:3-oxoacid CoA transferase. We would like to thank Dr. Yasushi Okazaki at Research Center for Genomic Medicine, Saitama Medical University for helpful discussion. We also thank Ms. Y. Yamashita, S. Sugimoto and K. Takabe for their technical assistance. This work was supported by research grants from the Ministry of Health, Labour, and Welfare (H. Saitsu, N. Matsumoto and N. Miyake), the Japan Science and Technology Agency (N. Matsumoto), the Strategic Research Program for Brain Sciences (to N. Matsumoto), a Grant-in-Aid for Scientific Research on Innovative Areas (Transcription Cycle) from the Ministry of Education, Culture, Sports, Science, and Technology of Japan (N. Matsumoto), a Grant-in-Aid for Scientific Research from the Japan Society for the Promotion of Science (to N. Matsumoto), a Grant-in-Aid for Young Scientists from the Japan Society for the Promotion of Science (H. Saitsu and N. Miyake), a grant from the 2012 Strategic Research Promotion of Yokohama City University (N. Matsumoto), and research grants from the Japan Epilepsy Research Foundation (H. Saitsu) and the Takeda Science Foundation (N. Matsumoto and N. Miyake).

Conflict of interest The authors declare that they have no conflict of interest.